Comparison of CT and chemical-shift MRI for differentiating thymoma from non-thymomatous conditions in myasthenia gravis: value of qualitative and quantitative assessment

Clinical Radiology 71 (2016) e157-e169 DOI: http://dx.doi.org/10.1016/j.crad.2015.12.009

A.M. Priola [a, *], S.M. Priola [a], D. Gned [a], M.T. Giraudo [b], A. Fornari [c], A. Veltri [a]

[a] Department of Diagnostic Imaging, San Luigi Gonzaga University Hospital, Regione Gonzole 10, 10043, Orbassano, Torino, Italy
[b] Department of Mathematics "Giuseppe Peano", University of Torino, Via Carlo Alberto 10, 10123, Torino, Italy
Department of Pathology, San Luigi Gonzaga University Hospital, Regione Gonzole 10, 10043, Orbassano, Torino, Italy

Comparison of CT and chemical-shift MRI for differentiating thymoma from non-thymomatous conditions in myasthenia gravis: value of qualitative and quantitative assessment

AIM: To evaluate the usefulness of computed tomography (CT) and chemical-shift magnetic resonance imaging (MRI) in patients with myasthenia gravis (MG) for differentiating thymoma (THY) from thymic lymphoid hyperplasia (TLH) and normal thymus (NT), and to determine which technique is more accurate.

MATERIALS AND METHODS: Eighty-three patients with generalised MG who underwent surgery were divided into the TLH/NT group (A; 65 patients) and THY group (B; 24 patients). Differences in qualitative characteristics and quantitative data (CT: radiodensity in Hounsfield units; MRI: signal intensity index [SII]) between groups were tested using Fisher's exact test and Student's t-test. Logistic regression models were estimated for both qualitative and quantitative analyses. At quantitative analysis, discrimination abilities were determined according to the area under the receiver operating characteristic (ROC) curve (AUROC) with computation of optimal cut-off points. The diagnostic accuracies of CT and MRI were compared using McNemar's test.

RESULTS: At qualitative assessment, MRI had higher accuracy than CT (96.4%, 80/83 and 86.7%, 72/83, respectively). At quantitative analysis, both the radiodensity and SII were significantly different between groups ($p<0.0001$). For CT, at quantitative assessment, the AUROC of the radiodensity in discriminating between groups was 0.904 (optimal cut-off point, 20 HU) with an accuracy of 77.1% (64/83). For MRI, the AUROC of the SII was 0.989 (optimal cut-off point, 7.766%) with an accuracy of 96.4% (80/83), which was significantly higher than CT ($p<0.0001$). By using optimal cut-off points for cases with an erroneous diagnosis at qualitative assessment, accuracy improved both for CT (89.2%, 74/83) and MRI (97.6%, 81/83).

Introduction

Diagnostic imaging is pivotal in myasthenia gravis (MG) for differentiating thymomas (THYs) from thymic lymphoid hyperplasia (TLH) and normal thymus (NT) because treat-ment strategies

are different, with surgery recommended at diagnosis solely in cases of THY.[1e5] Currently, computed tomography (CT) is considered the imaging technique of choice although it has limitations in differentiating TLH from THY when TLH does not present its typical triangular shape and appears as a focal mass with soft-tissue attenu-ation and no areas of fat.[2,6e 9] Conversely, magnetic reso-nance imaging (MRI) is not usually employed in clinical practice, although chemical-shift imaging could be helpful as it is more sensitive than CT for detecting fat in tissue.[2,7] It has been successfully used as a qualitative and quantitative technique, by calculating the signal intensity index (SII), to characterise lipid-poor adrenal adenomas, which are inde-terminate at CT, and for distinguishing thymic hyperplasia from anterior mediastinal tumours.[10e13] Chemical-shift imaging is based on the difference in precessional fre-quencies between water protons and fat protons, which causes a signal intensity loss on opposed-phase images compared with in-phase images in tissues composed of a fatewater admixture (e.g., NT and TLH), whereas no change in signal intensity occurs in tissues composed of a single proton species, either water only or fat only (e.g., tumours that usually do not include fat).[10e12]

Few long-standing studies have evaluated the accuracy of CT and MRI in patients with MG for differentiating THY from non-thymomatous conditions by using morphological and qualitative assessment with no quantitative data.[8,14,15] Furthermore, although two recent studies have demon-strated chemical-shift MRI as an effective technique for MG patients, no studies have compared the accuracy of CT and chemical-shift MRI in differentiating THY from TLH and NT by using both qualitative assessment and quantitative data.[16,17]

The aim of the present study was to compare the reli-ability of CT and chemical-shift MRI in patients with gener-alised MG for distinguishing THY from TLH and NT using morphological criteria and quantitative data (radiodensity [HU] for CT, SII for chemical-shift MRI), with the proposal of optimal cut-off point values for each quantitative parameter, and to determine which technique is more accurate.

Materials and methods

Patient population and reference diagnosis

The institutional review board approved the study, which was conducted from January 2007 through December 2014 and data were prospectively assessed. The inclusion criteria were as follows: (a) new onset of gener-alised MG; (b) definitive diagnosis based on histological findings from surgical resection; (c) no neo-adjuvant chemotherapeutic/radiotherapeutic treatment. Hence,

83 consecutive patients (42 men, 41 women; age range 14e71 years, median age 39 years, mean age_standard deviation 38.4_12.1 years; male: 18e68 years, 41years, 40.6_10.5 years; female: 14e71 years, 33 years, 36.2_13.3 years) were enrolled and evaluated with CT and MRI (mean time from imaging to surgery, 15.2 days; range, 1e37 days). Both imaging methods were performed at diagnosis of MG and at the end of the medical treatments, shortly before surgery, in patients who received symptomatic or immunomodulating treatments for MG followed by surgical resection. All patients were assigned to either the TLH/NT group (group A) or the THY group (group B) based on histological findings (Table 1). The median age of patients in group A was significantly lower than that of group B (p¼0.009), whereas no age difference was found between subgroups of each group (p¼0.26 and 0.89, respectively). For subgroups of each group, the median size of the NT and early THY were significantly lower than that of the TLH and advanced THY, respectively (TLH versus NT, p<0.0001; early versus advanced THY, p¼0.002).

Table 1

Demographic characteristics of the 83 enrolled patients[x].

Group and subgroup	n[a]	M/F ratio	Age (years)[b]	Size (mm)[c]
Group A[§]	65	31/34	35.5 (14,71)	12.0 (5,25)
Thymic lymphoid hyperplasia	48	22/26	39.0 (14,71)	13.0 (5,25)
Normal thymus	17	9/8	31.0 (18,49)	9.0 (5,12)
Group B[§]	24	16/8	41.5 (37,68)	29.0 (10,112)[d]
Early thymoma (stage I-II)	16	11/5	41.5 (27,68)	18.5 (10,49)[d]
Advanced thymoma (stage III-IV)	8	5/3	40.0 (30.68)	48.5 (29,112)

n, Number of findings (overall, 89 findings in 83 patients); M, male; F, female.

[a] Six patients are listed in both groups because of combined histological diagnosis of THY and TLH or NT after thymomectomy and extended thy-mectomy (thymic lymphoid hyperplasia and early thymoma in two patients, normal thymus and early thymoma in three patients, normal thymus and advanced thymoma in one patient).

[bc] Data are medians (ranges).

[c] Size is the thickness of the thymus, if triangular or quadrilateral shaped, measured as the maximum dimension perpendicular to the long axis of each lobe for group A and the maximal diameter of the lesion for group B or of the thymus if rounded or ovoid for group A, measured on transverse images.

[d] Mean size obtained in 22 out of 24 patients (for group B) and in 14 out of 16 patients (for the "early thymoma" subgroup) after excluding two patients with histological findings of microscopic

foci of thymoma, not appreciable at CT and chemical-shift MR, in a context of normal thymus and thymic lymphoid hyperplasia).

Imaging protocols

CT

CT examinations were performed using a 64-section CT system (Philips Brilliance, MX80001DT, Philips Medical Systems, Best, The Netherlands) in a single-breath hold at end-inspiration. Unenhanced CT was immediately followed by contrast-enhanced CT obtained 35 seconds after administration of 2 ml/kg of iopromide (370 mg iodine/ml;
Ultravist 370, Bayer Schering Pharma, Berlin, Germany; rate, 2.5 ml/s) if the unenhanced images showed a (a) round- or oval-shaped focal mass with soft-tissue attenuation or (b) triangular or quadrilateral-shaped thymus with soft-tissue or mixed attenuation in order to exclude a THY embedded in NT/TLH. Contrast-enhanced CT was avoided in patients with homogeneous fat appearance of the thymus at unen-hanced CT. Technical parameters included 120 kVp, 100e250 mAs with automatic dose modulation, pitch of 1, section thickness of 2 mm, contiguous section interval, and 512_512 matrix.

Chemical-shift MRI

MRI was obtained using a 1.5 T MRI unit (Intera-Achieva, Philips Healthcare, Best, The Netherlands), spanning the thoracic inlet to the cardiophrenic angle. All patients un-derwent transverse gradient-echo/T1-weighted dual-echo in- and opposed-phase imaging, using an anterior-to-posterior phase-encoding direction, in a single-breath hold; however, a left-to-right phase-encoding direction was used for quantitative evaluations in nine cases to avoid artefacts (due to heartbeat or flow motion in the great vessels) within the thymus or lesion, which were appre-ciable by using the anterior-to-posterior phase-encoding direction. Cardiac gating was not used. Imaging parameters did not change during the study period and included 240e400 mm field of view, 256_256 image matrix, 5 mm section thickness, 0e0.5 mm intersection gap, 90^{-} flip angle, 154 ms repetition time, and in-phase and opposed-phase echo-times of 4.6 and 2.3 ms. Axial T2-weighted MRI without and with fat suppression (386 and 415 ms repetition times and 100 and 80 ms echo times, respec-tively) was obtained for morphological analysis.

Table 2
Qualitative features of groups A and B with subgroups at computed tomography (CT) and magnetic resonance imaging (MRI).

Feature	Group A	Group B	*p*-Value[a]	TLH	NT	*p*-Value[a]	ETHY	ATHY	*p*-Value[a]
Location (mediastinum)									
Thoracic inlet	1	1		1	–		1	–	
Anterior superior	64	18	0.006	47	17	NS	11	7	NS
Anterior inferior	–	3		–	–		2	1	
Position									
Middle position	41	9		27	14		7	2	
Left sided	20	10	NS	17	3	NS	5	5	NS
Right sided	4	3		4	–		2	1	
Shape									
Focal mass	12	20	<0.0001	12	–	0.014	12	8	NS
Triangular/quadrilateral	53	2		36	17		2	–	
Shape (focal mass)									
Round	8	8	NS	8	–	–	6	2	NS
Oval	4	12		4	–		6	6	
Shape									
Triangular	50	2	NS	34	16	NS	2	–	–
Quadrilateral	3	–		2	1		–	–	
Margins									
Concave	32	–		17	15		–	–	
Convex	9	2	NS	9	–	NS	2	–	–
Straight	12	–		10	2		–	–	
Margins (focal mass)									
Smooth	12	11		12	–		8	3	
Irregular	–	3	0.017	–	–	–	1	2	NS
Lobulate	–	6		–	–		3	3	
Attenuation at CT (fat content)									
Completely fat	32	–		21	11		–	–	
Soft tissue with no fat	24	22	<0.0001	20	4	NS	14	8	NS
Mixed or partially fat	9	–		7	2		–	–	
Signal intensity loss at MRI									
Yes	61	–	<0.0001	44	17	NS	–	–	–
No	4	22		4	0		14	8	
Attenuation at unenhanced CT									
Homogeneous	58	11	0.00025	43	15	NS	8	3	NS
Heterogeneous	7	11		5	2		6	5	
Attenuation at enhanced CT [b]									
Homogeneous	31	11	<0.0001	26	6	NS	9	2	NS
Heterogeneous	2	11		1	–		5	6	
Calcifications at CT									
- Yes	–	9	<0.0001	–	–	–	5	4	NS
- No	65	13		48	17		9	4	
Cystic/necrotic component at CT									
- Yes	–	6	0.00014	–	–	–	4	2	NS
- No	65	16		48	17	–	10	6	
Cystic/necrotic component at MRI									
- Yes	–	8	<0.0001	–	–	–	6	2	NS
- No	65	14		48	17	–	8	6	

Data are number of findings (overall, 89 findings in 83 patients).

Group A comprised 65 findings. Group B comprised 22 out of 24 findings; two patients with final diagnosis of microscopic foci of thymoma not appreciable at CT and MRI are excluded from qualitative assessment.

TLH, thymic lymphoid hyperplasia (48 patients); NT, normal thymus (17 patients); ETHY, early thymoma (14 patients); ATHY, advanced thymoma (eight patients).

[a] Fisher's exact test; NS, not significant.

[b] Contrast-enhanced CT was performed in 33 out of 65 patients of group A with soft-tissue (24 patients) or mixed (nine patients) attenuation at unenhanced CT.

[c]

Image analysis

All CT and MRI images were analysed independently for qualitative and quantitative assessment by two different radiologists for each technique without knowledge of patients' identification and clinical/histological data. CT images were reviewed using the mediastinal window setting (level, 50 HU; width, 350 HU). For patients who received medical treatments for MG, no significant differences were found among examinations performed before and after medical treatments, and image analysis was car-ried out by using the last pair of examinations.

CT and chemical-shift MRI qualitative assessment

The qualitative parameters of the thymus or lesion evaluated at CT and MRI are listed in Table 2. After quali-tative analysis with either CT or MRI, each reader assigned a presumptive diagnosis of THY or NT/TLH based on the criteria reported in Table 3.

CT and chemical-shift MRI quantitative analysis

For CT, a region-of-interest (ROI) was manually drawn on the unenhanced axial images taking care to exclude peripheral areas (to avoid partial volume effects from adjacent structures), calcifications, cystic or necrotic com-ponents, and any region where streak or beam-hardening artefacts were appreciable, to avoid false reductions or in-creases in radiodensity values. For patients who received contrast medium, the ROI was placed on the area that visually exhibited the highest contrast enhancement and this was then mirrored on the corresponding unenhanced image in the same position. The difference in measured values on the enhanced and unenhanced images was considered the enhancement intensity.

For chemical-shift MRI, a ROI of the same size was placed over the same position within the tissue on both the in-phase and opposed-phase images in each case. The ROI placement was made first on the opposed-phase image to avoid the inclusion of areas of signal void at interfaces between fat-dominant and water-dominant tissues (India ink artefact), and then mirrored on the in-phase image in the exact same position avoiding cystic/necrotic components displayed on the corresponding T2-weighted images. The SII was determined by comparing the signal intensity of

tissue (tSI) on both the in-phase (in) and opposed-phase (op) im-ages using the equation: SII¼[(tSI$_{in}$etSI$_{op}$)/(tSI$_{in}$)]_100%.

Statistical analysis

For qualitative analysis, inter-rater agreement between the two readers was assessed using Cohen's kappa for each parameter evaluated at CT and MRI (k, range: 0e1). Subsequently, Cohen's kappa was used to evaluate inter-rater agreement between CT and MRI for each qualitative

Table 3
Computed tomography (CT) and magnetic resonance imaging (MRI) criteria for group assignment at qualitative assessment.

CT	At least one of the following criteria for the presumptive diagnosis of THY: (a) focal mass with homogeneous or heterogeneous soft-tissue attenuation and no evident fat infiltration at unenhanced CT (b) heterogeneous contrast enhancement (c) presence of calcifications and/or cystic/necrotic components regardless of morphology At least one of the following criteria for the presumptive diagnosis of NT/TLH: (a) triangular or quadrilateral shape even with soft-tissue attenuation on unenhanced CT, with convex, concave, or straight margins, but with no focal enlargements or lobulations (which may indicate the presence of an associated mass lesion) (b) homogeneous contrast enhancement for triangular/ quadrilateral-shaped thymuses with soft-tissue or mixed attenuation at unenhanced CT (c) focal mass with clear entire fat attenuation at unenhanced CT
MR	In addition to the same morphological criteria used for CT, specific MRI criteria for the presumptive diagnosis of THY: (a) presence of cystic/necrotic components on T2-weighted imaging regardless of morphological criteria (b) no signal intensity loss on opposed-phase images relative to in-phase images regardless of morphology[a] In addition to the same morphological criteria used for CT, specific MRI criterion for the presumptive diagnosis of NT/TLH: (a) homogeneous decrease in signal intensity on opposed-phase images relative to in-phase images regardless of morphology[a]

THY, thymoma; NT, normal thymus; TLH, thymic lymphoid hyperplasia.

[a] Such criteria were not used for patients under 16 years of age because chemical-shift MRI can detect physiological fatty infiltration within normal thymus in half of adolescents aged 11e15 years and in all patients over 16 years.[18]

parameter, and the CT characteristic was considered for further analyses for all parameters with excellent agree-ment (k>0.80), because of its better spatial resolution compared with MRI. Conversely, the parameter was considered separately for both CT and MRI for characteris-tics with k_0.8. Logistic regression models were used to estimate the probability that patients had THY or TLH/NT as a function of the chosen predictive variables. First, univar-iate analysis was performed using Fisher's exact test for each qualitative parameter; then, a multivariate logistic regression model corrected for patient age and gender was constructed using significant variables ($p<0.05$) in the univariate analysis. Lastly, diagnostic performance of CT and MRI was computed based on presumptive diagnoses assigned by the readers.

For quantitative analysis, data concerning radiodensity and SII were expressed as mean values _ standard de-viations and ranges according to the defined groups and subgroups because of their normal distribution at the Sha-piroeWilk test. The inter-reader agreement of radiodensity and SII measurements was assessed using the intraclass correlation coefficient (ICC; range: 0e1). Differences in radiodensity and SII levels between the groups and sub-groups were analysed using Student's t-test. Logistic regression models were estimated to evaluate the ability of the radiodensity and SII to discriminate between groups. The area under the receiver operating characteristic (ROC) curve (AUROC) was obtained and optimal cut-off points were determined using the Youden Index with computation of accuracy. Additional analyses aimed to control for age and gender as potential confounding factors were per-formed by including such variables in logistic regression models.

Lastly, considering both analyses, cases with erroneous presumptive CT or MRI diagnosis at qualitative assessment, were reassigned to one of the two groups based on optimal cut-off points determined at quantitative analysis for differentiating THY from NT/TLH in order to evaluate the improvement in accuracy by associating quantitative anal-ysis to qualitative evaluation.

The diagnostic performance of CT and MRI at qualitative, quantitative and both analyses was compared using McNemar's test and generalised score statistic. A p-value of <0.05 was considered indicative of a statistically significant difference.

Results

Interobserver variability for qualitative and quantitative assessment

For qualitative assessment, agreement between readers was excellent for CT and MRI findings (lower k¼0.91 for "cystic/necrotic component" at CT) and the characteristic reported by the more experienced reader was used for each case of discordance. Similarly, the agreement between CT and MRI for each characteristic was high (lower k¼0.87 for "margins") except for the "cystic/necrotic component" (k¼0.60). For quantitative evaluations, the inter-reader agreement was high with an ICC of 0.878 (95% confidence interval [CI]: 0.857e0.896) and 0.897 (95% CI: 0.886e0.918) for radio-density and SII, respectively. Hence, the mean radiodensity and SII value of the two readers was used for further analyses.

Qualitative analysis: reliability of CT and MRI in assessing the correct diagnosis

Table 4

Ability of qualitative assessment, quantitative analysis and both analyses for computed tomography (CT) and magnetic resonance imaging (MRI) in differen-tiating group A versus group B.

Technique	Sensitivity, %[a] (95% CI)	Specificity, %[a] (95% CI)	PPV, %[b] (95% CI)	NPV, %[b] (95% CI)	Accuracy, %[a] (95% CI)
Qualitative					
CT	83.3 (20/24) (68.4–98.2)	[c]89.2 (58/65) (82–96.8)	[c]74.1 (20/27) (57.5–90.6)	93.6 (58/62) (87.6–99-7)	87.6 (78/89) (79.4–93)
MR	91.7 (22/24) (81–100)	[c]96.9 (63/65) (93–100)	[c]91.7 (22/24) (81–100)	96.9 (63/65) (93–100)	96.6 (86/89) (89.1–98.3)
Quantitative					
CT (radiodensity, HU)	100 (22/22) (86.8–100)	[c]68.2 (45/66) (56.9–79.4)	[c]50 (21/42) (34.9–65.1)	97.8 (45/46) (93.6–100)	[c]75 (66/88) (65.7–84.2)
MRI (SII)	100 (22/22) (85.1–100)	[c]97 (64/66) (92.8–100)	[c]91.7 (22/24) (81–100)	100 (64/64) (94.3–100)	[c]98.9 (87/88) (97.8–100)
Both analyses					
CT	100 (22/22) (85.1–100)	[c]89.4 (59/66) (82–97)	[c]75.9 (22/29) (60.3–91.4)	100 (59/59) (93.9–100)	92 (81/88) (84.5–96.1)
MR	100 (22/22) (85.1–100)	[c]98.5 (65/66) (95.5–100)	[c]95.7 (22/23) (87.3–100)	100 (65/65) (94.4–100)	100 (88/88) (93.8–100)

Data are percentages of findings; numbers in brackets are referred to findings (overall, 89 findings in 83 patients).

For quantitative assessment and both analyses, two patients with final diagnosis of microscopic foci of thymoma embedded in normal thymus and thymic lymphoid hyperplasia are excluded from radiodensity and SII measurements for the thymoma group because of the absence of tissue with soft-tissue attenuation at CT and MRI (overall, 87 findings in 83 patients). Moreover, one subject with final diagnosis of thymic lymphoid hyperplasia is listed twice in group A because of CT and MRI appearance of ovoid solid tissue embedded in fatty infiltrated thymic tissue, each component

measured for quantitative analysis (88 findings overall: 66 findings in group A and 22 in group B in 83 patients), which suggested the erroneous hypothesis of small thymoma embedded in thymic lymphoid hyperplasia at qualitative analysis for both CT and MRI, and at quantitative assessment for CT but not for MRI (quantitative data of the solid component: CT: 23.5 HU; MRI: SII 10.41%).

A, thymic hyperplasia/normal thymus group; B, thymoma group. CI, confidence interval; HU, Hounsfield units; SII, signal intensity index.

[a] McNemar's test.

[b] Generalised score statistic.

[c] Statistically significant difference among CT and MR.

Table 4 reports the accuracy of CT and MRI for differ-entiating THY from NT/TLH. At qualitative assessment, the correct diagnosis was assessed in 86.7% (72/83 patients; 78/89 findings) and 96.4% (80/83 patients; 86/89 findings) of patients for CT and MRI, respectively. MRI was more reliable than CT and the difference was significant for specificity and positive predictive value (PPV; p¼0.048 and 0.04, respectively). Both techniques failed in two cases interpreted as NT/TLH at imaging, which presented with microscopic foci of THY at histology, and in a 71-year-old woman with TLH at surgery, which was inter-preted as THY embedded in TLH/NT at CT and MRI for the presence of ovoid tissue with soft-tissue attenuation and no signal intensity loss, embedded in a triangular-shaped fatty infiltrated thymus. In the last case, histology demonstrated a large area within a fatty infiltrated thymus characterised by many densely packed lymphoid follicles and limited fat. In addition, CT failed in seven cases of TLH, which were interpreted as THY because of their appearances as focal masses with soft-tissue atten-uation, which presented with signal intensity loss at chemical-shift MRI (Figs. 1 and 2). The mean size of these seven cases (15.7_5.4 mm) was not significantly different compared with the early THY subgroup (p¼0.11). The last case of discordance between CT and histology was a 27-year-old woman with non-advanced THY, who pre-sented with a triangular-shaped thymus with soft-tissue attenuation and homogeneous enhancement. At MRI, this case was correctly interpreted as THY because of its lack of signal decrease on opposed-phase images in a patient >16 years (Fig 3).

Qualitative analysis: differences in CT and MRI characteristics between groups and subgroups

Although univariate analysis demonstrates statistically significant differences among groups for

most of the qual-itative parameters (Table 2), at logistic multivariate re-gressions performed whenever possible, only shape (focal mass versus triangular/quadrilateral; odds ratio [OR]: 0.98; 95% CI: 89.4e99.8; p<0.0001) and unenhanced CT attenu-ation (OR: 0.927; 95% CI: 63.9e99.3, p¼0.0046) were sig-nificant for discrimination between groups, with probability of 2% and 7.3% of being NT/TLH if findings had focal shape and heterogeneous attenuation at unenhanced CT, respectively. Considering subgroups of each group, a significant difference was detected only for shape (focal versus triangular/quadrilateral) between subgroups of group A (TLH and NT; Table 2).

At qualitative analysis, 24/65 (37%) patients in the NT/ TLH group had tissue with soft-tissue attenuation at unenhanced CT (Fig 4). The mean age of patients with TLH/ NT and soft-tissue attenuation (TLH 29.6 years; NT 24 years; all, 28.3 years) was significantly lower than that of patients with TLH/NT and completely fat or mixed attenuation (TLH 40.2 years; NT, 36 years; all, 38.9 years; p<0.001).

For chemical-shift MRI, 4/65 (6.2%) patients in the TLH/ NT group had no appreciable signal intensity loss on the opposed-phase imaging compared with the in-phase im-aging. These patients comprised two adolescents (a 14-year-old female patient and a 15-year-old female patient, with SIIs of 0.35% and 7.77%, respectively), a 23-year-old man (SII of 12.67%), and a 71-year-old woman with an ovoid component of TLH with no signal decrease embedded in a triangular-shaped fatty infiltrated thymus (SII of 10.41%).

Quantitative analysis: differences in radiodensity and SII between groups and subgroups

Radiodensity (unenhanced CT) and SII differed signifi-cantly between group A and group B (p<0.0001), whereas insignificant differences in mean values of radiodensity and SII were found on comparing subgroups (Table 5, Fig 5aed).

Table 5

Mean radiodensity and intensity of enhancement at computed tomography (CT) and signal intensity index (SII) at magnetic resonance imaging (MRI) for groups A and B.

Parameter	Groups or subgroups		*p*-Value
Mean radiodensity and SII			
All groups	Group A [66[a]]	Group B [22[b]]	
Radiodensity	-1.64±24.32 (-44/38)	33.16±10.79 (20/58)	<0.0001
SII (%)	35.11±13.61 (0.35/66.11)	-0.27±3.94 (-7.95/6.37)	<0.0001
Group A	Thymic lymphoid hyperplasia [49[a]]	Normal thymus [17]	
Radiodensity	0.38±24.73 (-44/32)	-7.44±22.83 (-37/38)	0.2433
SII (%)	34.04±13.94 (0.35/60.4)	38.20±12.47 (19.61/66.11)	0.2593
Group B	Early thymoma [14[b]]	Advanced thymoma [8]	
Radiodensity	33.64±10.82 (20.5/58)	32.31±11.43 (20/54)	0.7928
SII (%)	-0.95±3.65 (-7.95/5.27)	0.91±4.4 (-5.13/6.37)	0.3323
Intensity of enhancement (mean value, HU) at CT[c]			
All groups	Group A[d] [33[a]]	Group B [22[b]]	
Radiodensity	11.28±6.87 (2.5/32)	18.68±10.5 (5.5/45)	0.0062
Group A	Thymic lymphoid hyperplasia [27[a]]	Normal thymus [6]	
Radiodensity	11.53±7.41 (2.5/32)	10.08±3.69 (7/16)	0.4909
Group B	Early thymoma [14[a]]	Advanced thymoma [8]	
Radiodensity	14.36±6.38 (5.5/26)	26.25±12.33 (11/45.5)	0.0312

A, thymic hyperplasia/normal thymus group; B, thymoma group; numbers in square brackets are number of findings.

Data are mean values ± standard deviations. Numbers in brackets are ranges.

[a] One subject with final diagnosis of thymic lymphoid hyperplasia is listed twice in group A and in the "thymic lymphoid hyperplasia" subgroup because of CT and MRI appearance of ovoid solid tissue embedded in fatty infiltrated thymic tissue, each component measured for quantitative analysis, that suggested the erroneous hypothesis of small thymoma embedded in thymic lymphoid hyperplasia.

[b] Two patients with final diagnosis of microscopic foci of thymoma embedded in normal thymus and thymic lymphoid hyperplasia are excluded from the "early thymoma" subgroup because of the absence of tissue with soft-tissue attenuation at CT and MRI.

[c] Intensity of enhancement is the difference in measured attenuation values on unenhanced and enhanced images.

[d] For group A, intensity of enhancement was evaluated in 33 patients who had at CT thymic tissue with soft-tissue attenuation (24 patients) or mixed attenuation (nine patients).

Adjusted logistic regression models demonstrated that both quantitative parameters were significantly correlated with the probability of finding THY, because the probability of tumour presence decreased with decreased radiodensity (OR per 1 HU increase, 1.24; 95% CI: 1.32e1.17) and decreased with increased SII (OR per 1% increase, 0.64; 95% CI: 0.71e0.58). Therefore, an increase in unitary value in radiodensity and SII for fixed age and gender leads to an increase of 24% and reduction of 36%, respectively, in the probability of finding THY.

Table 4 reports the accuracy of CT and MRI for differen-tiating THY from NT/TLH employing the optimal cut-off point as a diagnostic criterion. The AUROC of radiodensity in discriminating between groups was 0.904 (95% CI: 0.841e0.967) with an optimal cut-off point of 20 HU (You-den Index J¼0.621; Fig 6a). Applying this cut-off point, the correct diagnosis was assessed in 75% (66/88) of CT findings (64/83 patients, 77.1%). The AUROC of SII in discriminating between groups was 0.989 (95% CI: 0.972e1) with an optimal cut-off point of 7.766% (Youden Index J¼0.804; Fig 6b). Applying this cut-off point, the correct diagnosis was assessed in 98.9% (87/88) of MRI findings (80/83 pa-tients, 96.4%). MRI was more reliable than CT and the dif-ference was statistically significant for specificity, PPV, and accuracy ($p<0.0001$). Lastly, at contrast-enhanced CT performed in 55 patients, the intensity of enhancement was significantly different between groups, being higher in THY compared with NT/ TLH (p¼0.006; Table 5, Fig 5e). The AUROC of intensity of enhancement in discriminating between groups was 0.733 (95% CI: 0.599e0.868). The optimal cut-off point was identified as an increase of 14 HU on contrast-enhanced CT compared with the unenhanced image (Youden Index J¼0.673). Applying this cut-off point, the correct diagnosis was assessed in 77.2% (44/57, 95% CI: 66.1e88.3%) of CT findings (42/55 patients, 76.4%) with a sensitivity and specificity of 63% and 76%, respectively. For subgroups, the intensity of enhancement was significantly different for group B, being higher in advanced THY compared with early THY, but not for group A (Table 5, Fig 5f).

Qualitative and quantitative analysis: reliability of CT and MRI in assessing the correct diagnosis

Table 4 reports the accuracy of CT and MRI in differenti-ating THY from NT/TLH by integrating quantitative data with qualitative evaluation. For CT, two patients with a final diagnosis of TLH, who were assigned to the THY group because of evidence of a small mass with focal shape and soft-tissue attenuation at qualitative assessment, were subsequently assigned to the NT/TLH group after quantita-tive evaluation as the tissue had values >20 HU. Thus, by using both qualitative and quantitative CT assessment, the correct diagnosis was established in 89.2% (74/83 patients, 81/88

findings) of patients. Similarly, for MRI, the optimal cut-off point obtained for the SII established the correct diagnosis in the 71-year-old woman with TLH at surgery because the solid component embedded in thymic tissue with no signal intensity loss at visual assessment had a SII of 10.41%. Hence, for MRI by using both analyses, the correct diagnosis was assessed in 97.6% (81/83 patients, 88/88 findings). MRI was more reliable than CT and the difference was significant for specificity and PPV (p¼0.014 and 0.006, respectively).

Discussion

In the present study, chemical-shift MRI was found to have higher accuracy compared with CT for qualitative and quantitative assessment in patients with MG. This is the first study to compare CT and MRI for qualitative and quantitative distinction of THY from NT and TLH.

Qualitative assessment

In spite of the technical development in CT, regarding qualitative assessment, similar accuracy data were obtained to the study of Pirronti et al.[15] (86.7% versus 83%), suggesting limitations in qualitative analysis of CT. More-over, although Batra et al.[14] demonstrated that MRI added no significant information to results obtained with CT, in the present study at qualitative assessment, MRI (with the addition of chemical-shift imaging) was more reliable than CT in discriminating THY from non-thymomatous condi-tions, with an overall accuracy of 96.4%. In the present cohort, most of cases in which CT failed (7/11, 64%) were TLH with a focal appearance and soft-tissue attenuation, a condition that was reported in 20% of patients with MG by Nicolau et al.[8] and which is indistinguishable from THY if no obvious fat infiltration is seen.[8,9] Furthermore, in the pre-sent study, size did not help distinction because, although the mean size of focal TLH with soft-tissue appearance at CT was smaller compared with early THY subgroup (15.7 versus 18.5 mm), this size difference was not significant.

Regardless of morphology, patients who have NT or TLH with soft-tissue attenuation at CT, a condition that typically occurs in young adulthood, may be problematic to evaluate because a small THY with similar solid attenuation may be hidden within the normal/hyperplastic thymus.[2,15,19e25] In the present cohort, 37% of patients in the NT/TLH group had tissue with entirely solid attenuation. In such cases, chemical-shift MRI may represent a useful problem-solving technique because of its better ability to detect even microscopic amounts of fat within the tissue.[11,26e30] Indeed, in the

present study, only 6% of patients with NT/TLH had no signal intensity loss at visual assessment, and among them none of the seven cases with focal TLH and soft-tissue attenuation at CT was included. Moreover, MRI enable the correct diagnosis in one case of triangular-shaped THY, which was interpreted as a diffusely enlarged thymus with soft-tissue attenuation at CT.[11] Such high reliability of chemical-shift MRI in detecting fat in tissue is similar to that of previous studies that evaluated normal/hyperplastic thymus and anterior mediastinal tumours in mixed pop-ulations of different diseases.[11,12,16,17,31,32] Nevertheless, visual assessment of signal intensity loss at chemical-shift MRI for characterising NT and TLH has limitations because its inability to detect fat in NT of adolescents and children <16 years (two cases in the present cohort) and in sporadic cases of adults with NT, TLH, or rebound hyperplasia previously reported in literature.[12,18,31,33,34] One case of partially non-suppressing TLH occurred in a 71-year-old woman because of extensive areas of lymphoid follicles with no fatty infil-tration at histology. In such cases, diffusion-weighted im-aging may be helpful by demonstrating unrestricted diffusion in a normal or hyperplastic thymus.[17,34] Indeed, because diffusion-weighted imaging provides information related to the cell density and cellular architecture of tissues based on the random translational molecular motion of water molecules, it has been used in different organs for distinguishing benign from malignant lesions through the measurement of the apparent diffusion coefficient (ADC), which is significantly lower in malignant tumours (e.g., high-grade THY and mediastinal lymphoma) compared with normal tissues or hyperplastic thymus (e.g., NT and TLH, which do not suppress on opposed-phase imaging because of the low lipid content within the thymus, as generally seen in young patients).[35e38] Diffusion-weighted imaging does have limitations because of overlapping values among benign conditions (e.g., NT and TLH) and low-grade or non-advanced THYs that have unrestricted diffusion and high ADC values.[39e41]

Quantitative analysis: unenhanced CT and MRI

The main advantage of quantitative imaging is in obtaining quantitative data in addition to qualitative and morphological assessment, which should result in improved characterisation of tissues.[35,36] Nevertheless, for chemical-shift MRI, although quantitative analysis im-proves characterisation of the thymus and lesions of the anterior mediastinum compared with qualitative analysis, it is not routinely performed because visual analysis is easier to apply than quantitative assessment. The present study demonstrates that quantitative assessment of CT and MRI may be used as an independent predictive factor for differentiating THY from NT/TLH in MG, although the ac-curacy of chemical-shift MRI is significantly higher than CT. For MRI, three out of four patients

with no visual decrease in signal intensity of TLH had SII higher than the optimal cut-off point value of 7.766% for differentiating NT/TLH from THY, whereas the remaining case was a 14-year-old female patient with TLH and a SII of 0.35%. This finding of imperfect reliability of chemical-shift MRI by visual assessment, with discordance between qualitative analysis (no visually appreciable signal loss) and quantitative assessment (the SII was higher than the optimal cut-off point to identify NT/ TLH), is similar to that found in some studies evaluating adrenal adenomas with chemical-shift MRI; this discor-dance was reported in 7% of cases compared with 5% (3/65) of patients in the NT/TLH group obtained from the present cohort.[10,42e44] Hence, especially for MRI, quantitative analysis should always be performed alongside qualitative assessment because quantitative analysis alone or in com-bination with qualitative evaluation has higher accuracy compared with qualitative evaluation alone and could be helpful in cases of NT/TLH presenting with no appreciable signal intensity loss. Conversely, for CT, quantitative evaluation did not show similar excellent predictive ability for differentiating THY from NT/TLH; it had a significantly lower accuracy compared with the qualitative analysis (77.1% versus 86.7%).

Quantitative analysis: unenhanced and contrast-enhanced CT

For unenhanced and contrast-enhanced CT, no difference was found in the attenuation of the NT compared with TLH. Conversely, in their cohort of 15 patients, Araki et al.[45] re-ported higher attenuation of the thymus in the TLH group compared with the true hyperplasia group (a condition indistinguishable from NT at histology) at contrast-enhanced CT, although these data were not confirmed at unenhanced CT. In the present study, a significantly higher intensity of enhancement was demonstrated for the NT/TLH group compared with the THY group and for advanced THY compared with early THY. The latter finding suggests that neoangiogenesis, which is generally related to the aggres-siveness of tumours, could be higher in advanced THY.[46e48] Moreover, the intensity of enhancement could be helpful in identifying cases of focal TLH with soft-tissue attenuation at visual analysis and mean values of attenuation higher than 20 HU at unenhanced CT by using the optimal cut-off point of 14 HU for this discrimination.

Limitations and conclusions

There are limitations to the present study. First, in order to obtain histological examination as reference standard of diagnosis, only patients who underwent surgery were included. Hence, among patients with an atrophic or normal-sized thymus at imaging who were not surgically treated, other cases of microscopic THY may have been excluded. Second, although the proposed cut-off values

of CT and MRI showed good accuracy, these results were derived from the data analysed and need to be validated in independent samples of patients.

In conclusion, chemical-shift MRI is more reliable than CT for distinguishing THY from NT/TLH and could replace CT in everyday clinical practice for evaluating patients with MG.

References

1. Conti-Fine BM, Milani M, Kaminski HJ. Myasthenia gravis: past, present, and future. J Clin Invest 2006;116:2843e54.
2. Priola AM, Priola SM. Imaging of thymus in myasthenia gravis: from thymic hyperplasia to thymic tumor. Clin Radiol 2014;69:e230e45.
3. Diaz A, Black E, Dunning J. Is thymectomy in non-thymomatous myasthenia gravis of any benefit? Interact Cardiovasc Thorac Surg 2014;18:381e9.
4. Ruffini E, Van Raemdonck D, Detterbeck F, et al. European Society of Thoracic Surgeons Thymic Questionnaire Working Group. Management of thymic tumors: a survey of current practice among members of the European Society of Thoracic Surgeons. J Thorac Oncol 2011;6:614e23.
5. Silvestri NJ, Wolfe GI. Myasthenia gravis. Semin Neurol 2012;32:215e26.
6. Spillane J, Higham E, Kullmann DM. Myasthenia gravis. BMJ 2012;345:e8497.
7. Priola AM, Priola SM, Giraudo MT. Usefulness of CT in differentiating lymphoid thymic hyperplasia from true thymic hyperplasia: added value of thymic measurements and CT attenuation. AJR Am J Roentgenol 2015;204:W113e4.
8. Nicolau S, Muller NL, Li DKB, et al. Thymus in myasthenia gravis: com-parison of CT and pathologic findings and clinical outcome after thy-mectomy. Radiology 1996;200:471e4.
9. Nakagawa M, Hara M, Itoh M, et al. Nodular thymic lymphoid follicular hyperplasia mimicking thymoma. Clin Imaging 2008;32:54e7.
10. Park BK, Kim CK, Kim B, et al. Comparison of delayed enhanced CT and chemical shift MRI for evaluating hyperattenuating incidental adrenal masses. Radiology 2007;243:760e5.
11. Inaoka T, Takahashi K, Mineta M, et al. Thymic hyperplasia and thymus gland tumors: differentiation with chemical shift MRI imaging. Radi-ology 2007;243:869e76.
12. Priola AM, Priola SM, Ciccone G, et al. Differentiation of rebound and lymphoid thymic hyperplasia from anterior mediastinal tumors with dual-echo chemical-shift magnetic resonance imaging in adulthood: reliability of the chemical-shift ratio and signal-intensity index. Radi-ology 2015;274:238e49.
13. Priola AM, Priola SM. Primary mediastinal Hodgkin lymphoma and rebound thymic hyperplasia: differentiation with chemical-shift mag-netic resonance imaging after treatment. Int J Hematol 2009;90:8e10.
14. Batra P, Herrmann Jr C, Mulder D. Mediastinal imaging in myasthenia gravis: correlation of chest radiography, CT, MR, and surgical findings.
AJR Am J Roentgenol 1987;148:515e9.
15. Pirronti T, Rinaldi P, Batocchi AP, et al. Thymic lesions and myasthenia gravis. Diagnosis based on mediastinal imaging and pathological find-ings. Acta Radiol 2002;43:380e4.
16. Popa GA, Preda EM, Scheau C, et al. Updates in MRI characterisation of the thymus in myasthenic patients. J Med Life 2012;5:206e10.
17. Priola AM, Priola SM, Giraudo MT, et al. Chemical-shift and diffusion-weighted magnetic resonance imaging of thymus in myasthenia gravis: usefulness of quantitative assessment. Invest Radiol 2015;50:228e38.
18. Inaoka T, Takahashi K, Iwata K, et al. Evaluation of normal fatty replacement of the thymus with chemical-shift MRI imaging for iden-tification of the normal thymus. J Magn Reson Imaging 2005;22:341e6.
19. Lewis RA. Myasthenia gravis: new therapeutic approaches based on pathoph yearsiology. J Neurol Sci 2013;333:93e8.
20. Priola AM, Priola SM, Cardinale L, et al. The anterior mediastinum: diseases. Radiol Med 2006;111:312e42.

21. Skeie GO, Apostolski S, Evoli A, et al. Guidelines for treatment of auto-immune neuromuscular transmission disorders. Eur J Neurol 2010;17:893e902.

22. Gronseth GS, Barohn RJ. Thymectomy for non-thymomatous autoim-mune myasthenia gravis (an evidence-based review). Neurology 2000;55:7e15.

23. Mizuno T, Hashimoto T, Masaoka A, et al. Thymic follicular hyperplasia manifested as an anterior mediastinal mass. Jpn J Surg 1997;27:275e7.

24. Marom EM, Rosado-de-Christenson ML, Bruzzi JF, et al. Standard report terms for chest computed tomography reports of anterior mediastinal masses suspicious for thymoma. J Thorac Oncol 2011;6:S1717e23.
25. Benveniste MF, Moran CA, Mawlawi O, et al. FDG PET-CT aids in the preoperative assessment of patients with newly diagnosed thymic epithelial malignancies. J Thorac Oncol 2013;8:502e10.
26. Hood MN, Vincent B, Smirniotopoulos JG, et al. Chemical shift: the artifact and clinical tool revisited. RadioGraphics 1999;19:357e71.
27. Pokharel SS, Macura KJ, Kamel IR, et al. Current MRI imaging lipid detection techniques for diagnosis of lesions in the abdomen and pelvis.
RadioGraphics 2013;33:681e702.
28. Hughes Cassidy F, Yokoo T, Aganovic L, et al. Fatty liver disease: MR imaging techniques for the detection and quantification of liver stea-tosis. RadioGraphics 2009;29:231e60.
29. Priola SM, Priola AM, Cardinale L, et al. The anterior mediastinum: anatomy and imaging procedures. Radiol Med 2006;111:295e311.
30. Priola AM, Galetto G, Priola SM. Diagnostic and functional imaging of thymic and mediastinal involvement in lymphoproliferative disorders. Clin Imaging 2014;38:771e84.
31. Takahashi K, Inaoka T, Murukami N, et al. Characterization of the normal and hyperplastic thymus by chemical-shift MR imaging. AJR Am J Roentgenol 2003;180:1265e9.
32. Priola AM, Priola SM. Chemical-shift MRI of rebound thymic hyperplasia with unusual appearance and intense ^{18}F-FDG uptake in adulthood: report of two cases. Clin Imaging 2014;38:739e42.
33. Ackman JB, Mino-Kenudson M, Morse CR. Nonsuppressing normal thymus on chemical shift magnetic resonance imaging in a young woman. J Thoracic Imaging 2012;27:196e8.
34. Priola AM, Gned D, Marci V, et al. Diffusion-weighted MRI in a case of nonsuppressing rebound thymic hyperplasia on chemical-shift MRI. Jpn J Radiol 2015;33:158e63.
35. Padhani AR, Guoying L, Mu-Koh D, et al. Diffusion-weighted magnetic resonance imaging as a cancer biomarker: consensus and recommen-dations. Neoplasia 2009;11:102e25.
36. Koh DM, Collins DJ. Diffusion-weighted MRI in the body: applications and challenges in oncology. AJR Am J Roentgenol 2007;188:1622e35.
37. Gum€us¸€ tas¸ S, Inan N, Sarisoy HT, et al. Malignant versus benign medi-astinal lesions: quantitative assessment with diffusion weighted MRI imaging. Eur Radiol 2011;21:2255e60.

38. Seki S, Koyama H, Ohno Y, et al. Diffusion-weighted MRI imaging versus multi-detector row-CT: direct comparison of capability for assessment of management needs for anterior mediastinal solitary tumors. Eur J Radiol 2014;83:835e42.

39. Abdel Razek AA, Khairy M, Nada N. Diffusion-weighted MRI imaging in thymic epithelial tumors: correlation with World Health Organization classification and clinical staging. Radiology 2015;273:268e75.
40. Priola AM, Priola SM. Usefulness of diffusion-weighted MRI imaging in predicting MasaokaeKoga clinical staging of thymic epithelial tu-mors by using the apparent diffusion coefficient. Radiology 2015;274:936e7.

41. Priola AM, Priola SM, Giraudo MT, et al. Diffusion-weighted magnetic resonance imaging of thymoma: ability of the apparent diffusion coef-ficient in predicting the World Health Organization (WHO) classification and the MasaokaeKoga staging system and its prognostic significance on disease-free survival. Eur Radiol 2016. http://dx.doi.org/10.1007/ s00330-015-4031-6. in press.

42. Israel GM, Korobkin M, Wang C, et al. Comparison of unenhanced CT and chemical shift MRI in evaluating lipid-

rich adrenal adenomas. AJR Am J Roentgenol 2004;183:215e9.
43. Haider MA, Ghai S, Jhaveri K, et al. Chemical shift MR imaging of hyperattenuating (>10 HU) adrenal masses: does it still have a role? Radiology 2004;231:711e6.
44. Fujiyoshi F, Nakajo M, Fukukura Y, et al. Characterization of adrenal tumors by chemical shift fast low angle shot MR imaging: comparison of four methods of quantitative evaluation. AJR Am J Roentgenol 2003;180:1649e57.
45. Araki T, Sholl LM, Gerbaudo VH, et al. Imaging characteristics of path-ologically proven thymic hyperplasia: identifying features that can differentiate true from lymphoid hyperplasia. AJR Am J Roentgenol 2014;202:471e8.
46. Priola AM, Priola SM, Di Franco M, et al. Computed tomography and thymoma: distinctive findings in invasive and noninvasive thymoma and predictive features of recurrence. Radiol Med 2010;115:1e21.
47. McErlean A, Huang J, Zabor EC, et al. Distinguishing benign thymic le-sions from early-stage thymic malignancies on computed tomography. J Thorac Oncol 2013;8:967e73.
48. Marom EM, Milito MA, Moran CA, et al. Computed tomography findings predicting invasiveness of thymoma. J Thorac Oncol 2011;6:1274e81.

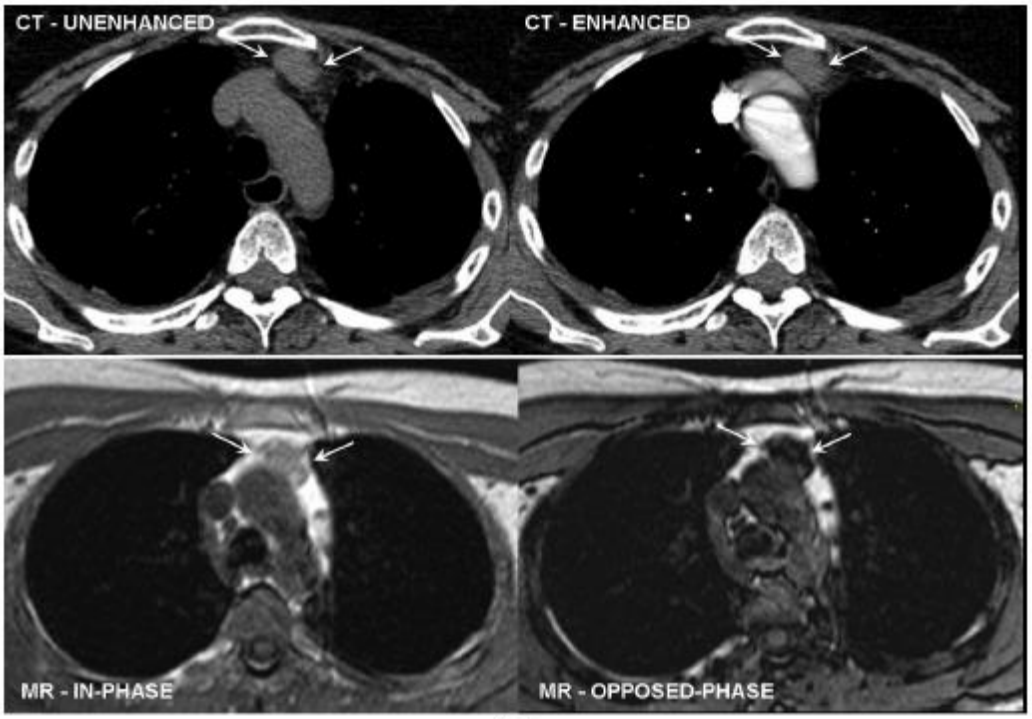
CT - UNENHANCED
CT - ENHANCED
MR - IN-PHASE
MR - OPPOSED-PHASE

(a)

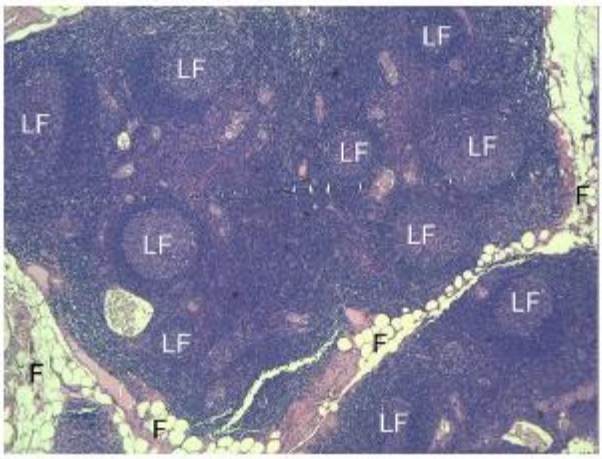
LF
LF
LF
LF
LF
F
LF
LF
LF
LF
F
F
F
LF

(b)

Figure 1

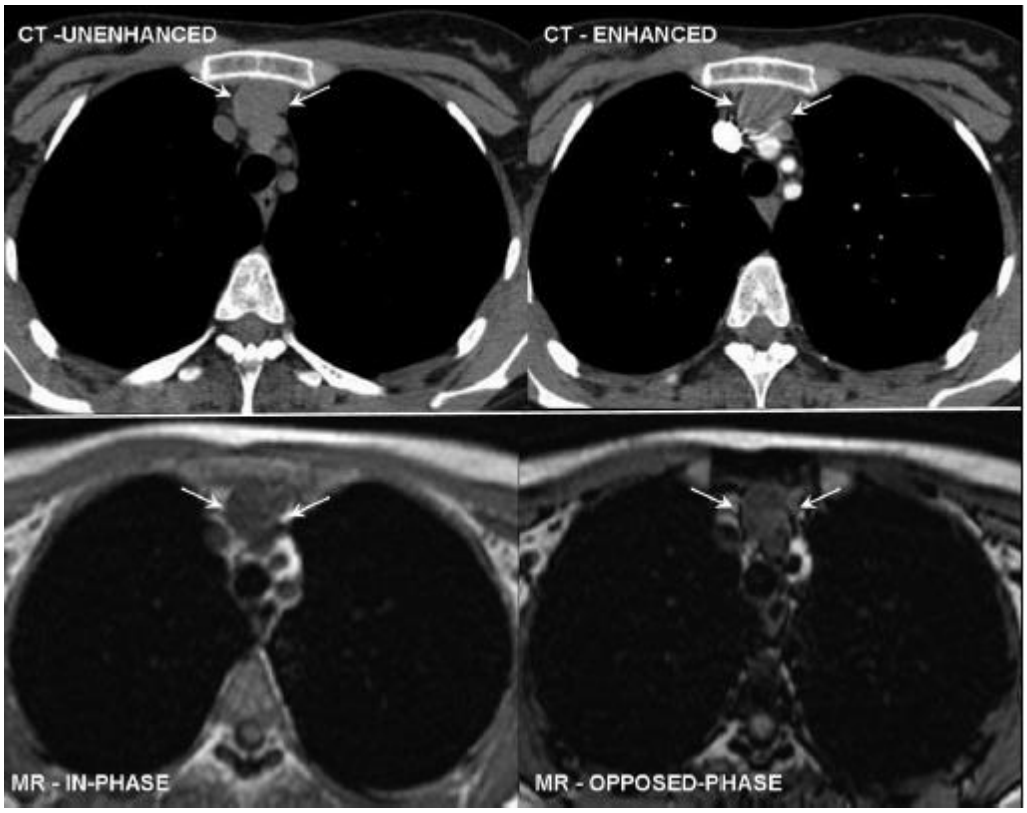

Figure 2

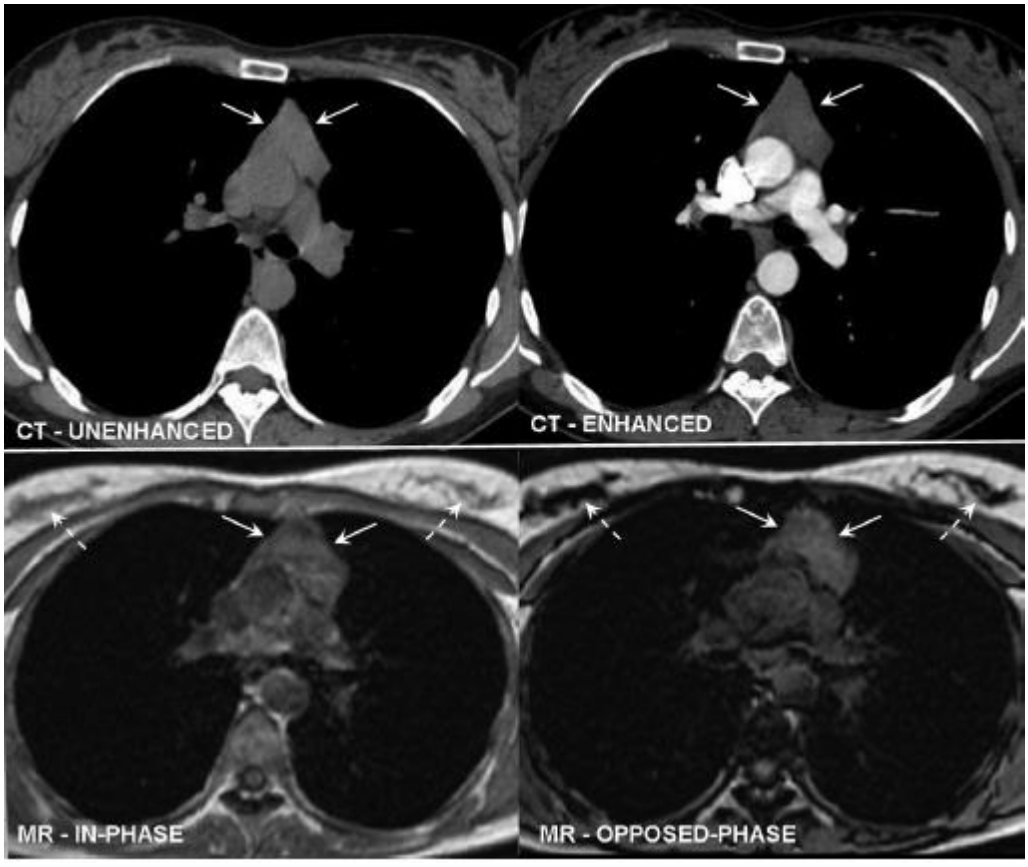

Figure 3

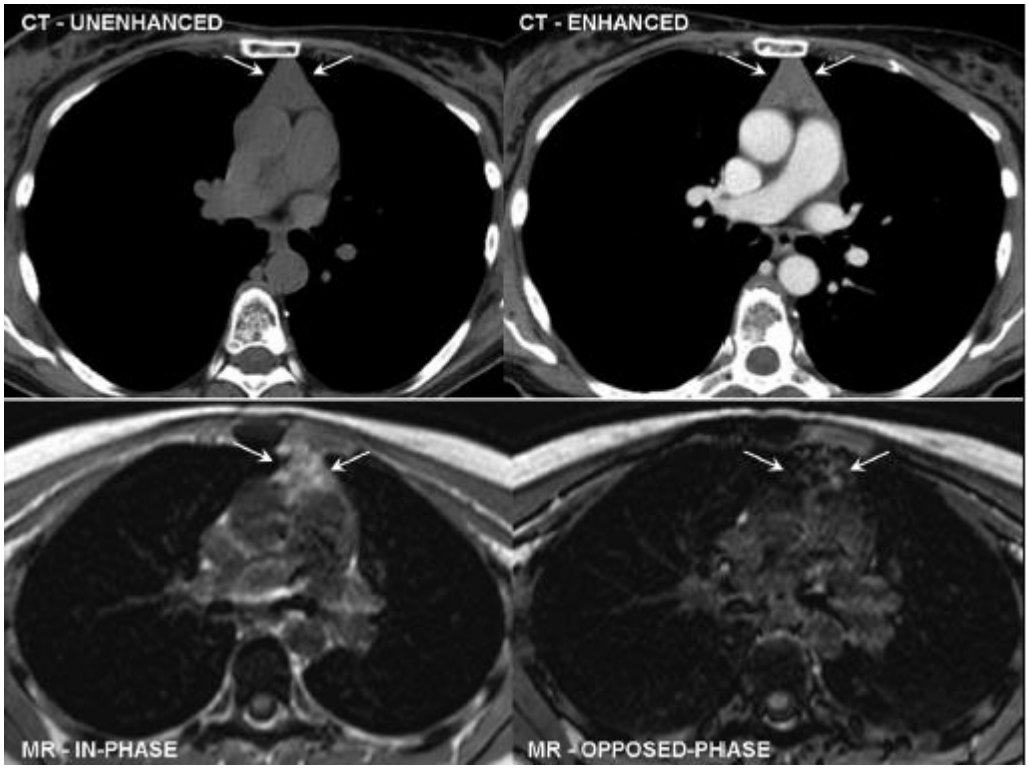

Figure 4

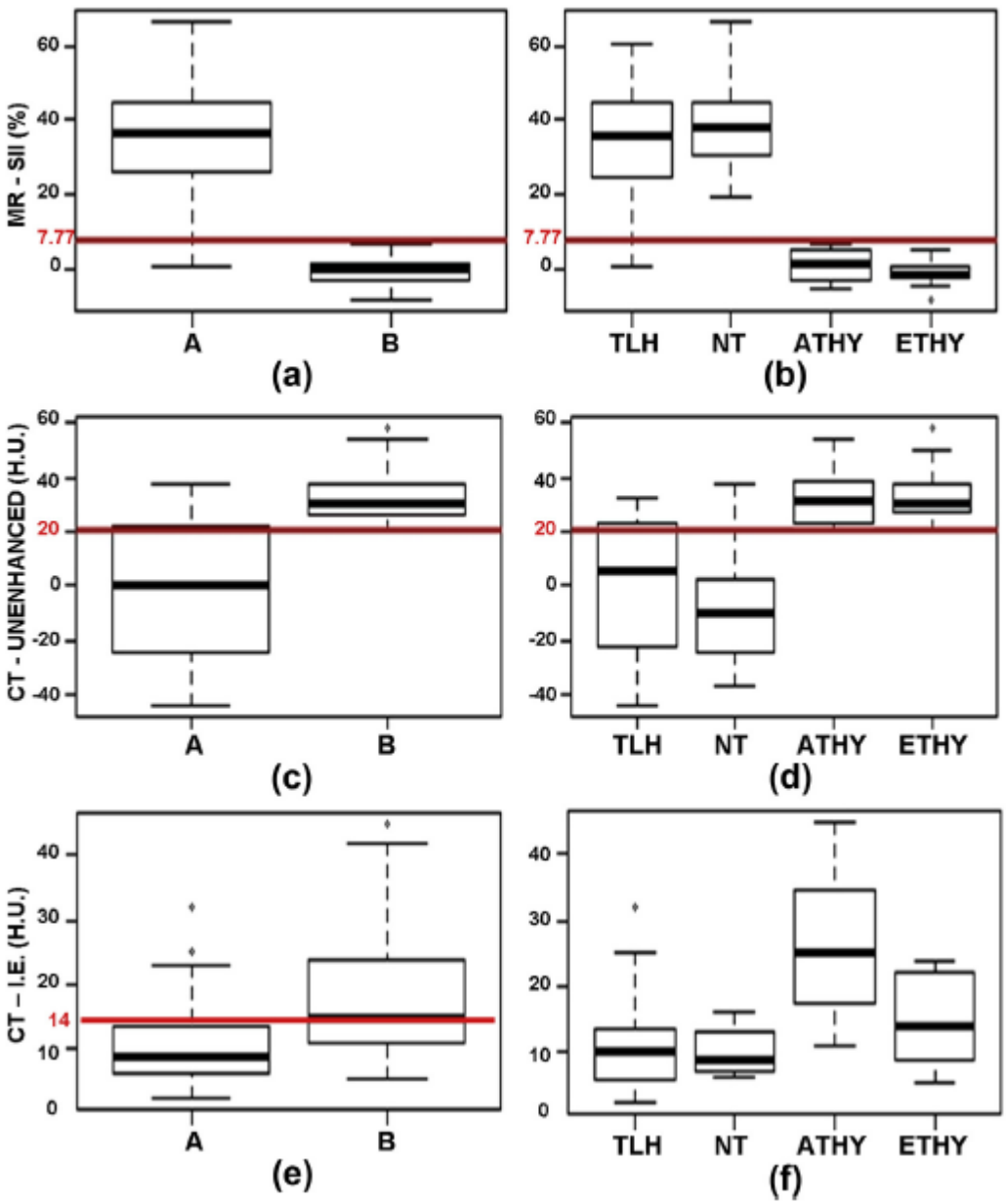
MR - SII (%)
60
40
20
7.77
0
A
B
(a)
TLH
NT
ATHY
ETHY
(b)
CT - UNENHANCED (H.U.)
20
-20
-40
(c)
(d)
CT – I.E. (H.U.)
30
14
10
(e)
(f)

Figure 5

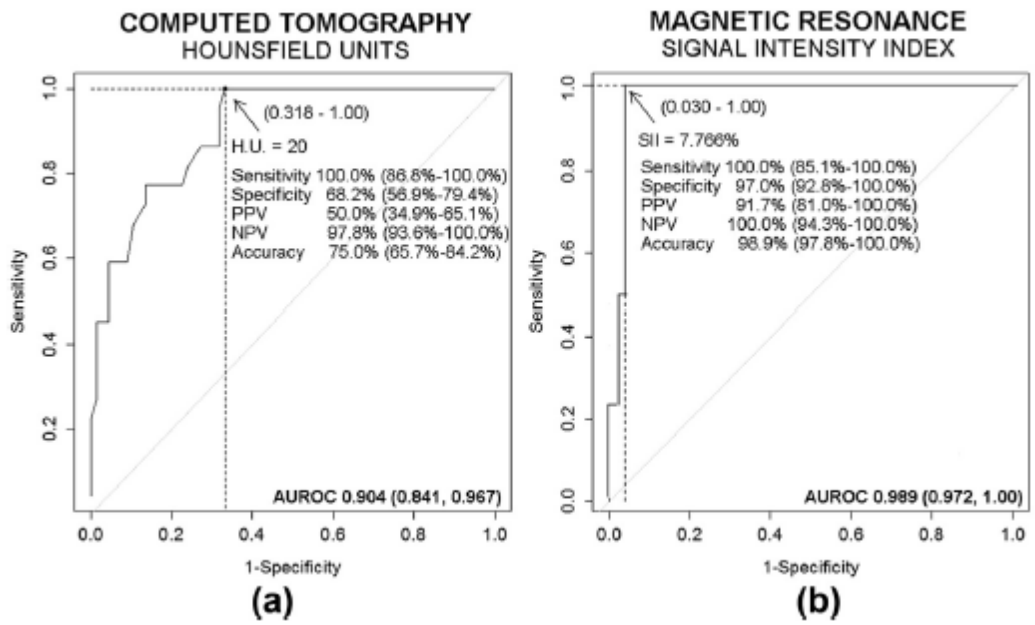
COMPUTED TOMOGRAPHY
HOUNSFIELD UNITS
(0.318 - 1.00)
H.U. = 20
Sensitivity 100.0% (86.6%-100.0%)
Specificity 68.2% (56.9%-79.4%)
PPV 50.0% (34.9%-65.1%)
NPV 97.8% (93.6%-100.0%)
Accuracy 75.0% (65.7%-84.2%)
AUROC 0.904 (0.841, 0.967)
Sensitivity
1-Specificity
(a)
MAGNETIC RESONANCE
SIGNAL INTENSITY INDEX
(0.030 - 1.00)
SII = 7.766%
Sensitivity 100.0% (85.1%-100.0%)
Specificity 97.0% (92.8%-100.0%)
PPV 91.7% (81.0%-100.0%)
NPV 100.0% (94.3%-100.0%)
Accuracy 98.9% (97.8%-100.0%)
AUROC 0.989 (0.972, 1.00)
Sensitivity
1-Specificity
(b)

Figure 6

Figure legends

Figure 1 A 31-year-old man with TLH. (a, upper images) Unenhanced CT reveals an oval-shaped small mass (arrows) anterior to the aortic arch and brachiocephalic vein, measuring 2 cm in maximal diameter, which exhibits homogeneous soft-tissue attenuation (mean densitometric value, 31 HU), similar to that of muscles, and mild contrast enhancement (intensity of enhancement, 6 HU). This appearance mimics a small THY and is similar to that depicted in Fig 2. (a, lower images) Chemical-shift MRI detects signal intensity loss of the tissue on opposed-phase images relative to in-phase images (arrows), consistent with a fatty component within the tissue, which suggests the diagnosis of TLH with focal appearance. (b) Photomicrograph of a representative histological section demonstrates minimally fatty infiltration of the thymic tissue, with limited areas of fat cells (F), and many lymphoid follicles (LF) densely packed and characterised by prominent germinal centres (haematoxylin and eosin stain, original magnification _40).

Figure 2 A 49-year-old woman with early THY. Unenhanced chest CT (upper images) shows a 2.5 cm round mass (arrows) in the anterior superior mediastinum, with smooth and well-demarcated margins, which presents soft-tissue attenuation (mean densitometric value, 45 HU), similar to that of muscles and vessels, and homogeneous enhancement after contrast medium administration (intensity of enhancement, 15 HU), an appearance that suggests the diagnosis of small THY and is morphologically similar to the case depicted in Fig 1a. Chemical-shift MRI (lower images) demonstrates no change in signal intensity of the mass on opposed-phase images relative to in-phase images (arrows), consistent with the absence of fat within the tissue. This suggestion is confirmed at quantitative assessment (SII¼0.62%) and strengthens the hypothesis of THY.

Figure 3 A 27-year-old woman with early THY. Unenhanced CT (upper images) obtained at the level of the pulmonary arteries reveals a diffusely enlarged triangular-shaped thymus (arrows; lobe thickness, 2 cm) with arrowhead morphology and soft-tissue attenuation (mean densitometric value, 29.5 HU), similar to that of muscles and vessels, which presents slight and homogeneous contrast enhancement (intensity of enhance-ment, 7.5 HU). These findings suggest the presumptive diagnosis of TLH with soft-tissue attenuation. Chemical-shift MRI (lower images) shows no decrease in signal intensity of the tissue on opposed-phase images relative to in-phase images (arrows), consistent with the absence of fatty infiltration. At quantitative evaluation, the SII of 1.67% confirms the absence of fat and suggests the hypothesis of a triangular-shaped THY. Conversely, breast tissue presents homogeneous signal intensity loss on opposed-phase images compared with in-phase images (dotted arrows), which reflects the fatewater admixture within the gland.

Figure 4 A 26-year-old woman with TLH. Unenhanced CT (upper images) obtained at the level of the pulmonary trunk demonstrates a normal-sized triangular-shaped thymus (arrows; lobe thickness, 1.2 cm) with arrowhead morphology, straight margins, and soft-tissue attenuation (mean densitometric value, 25 HU) which presents slight and homogeneous contrast enhancement (intensity of enhancement, 8 HU). These findings suggest the presumptive diagnosis of NT or normal-sized TLH. Chemical-shift MRI (lower images) shows a remarkable homogeneous decrease in signal intensity of thymus on opposed-phase images relative to in-phase images (arrows), consistent with fatty infiltration within tissue. This finding is confirmed at quantitative analysis (SII

of 21%).

Figure 5 Box-and-whiskers plots show the SII (a, b), radiodensity at unenhanced CT (c, d), and intensity of enhancement (IE) at contrast-enhanced CT (e, f) values for all cases divided into groups (a, c, e) and subgroups (b, d, f). The subgroups include patients with TLH and NT for group A, and patients with advanced THY (ATHY) and early THY (ETHY) for group B. The boxes represent data from the 25th to the 75th percentile. The horizontal line inside the boxes is the median (50^{th} percentile). The vertical lines with whiskers indicate the range from the largest to smallest observed data point, within 1.5_ interquartile range (IQR) of the higher and lower quartile, respectively. The values outside this range (CT unenhanced, group B and ETHY; CT IE, group A and TLH, group B) are displayed as individual points. The continuous horizontal thick line in the graphs shows the optimal cut-off value for discrimination among groups deriving from the ROC analysis. For groups, a larger overlap zone is appreciable for unenhanced CT (from 20 to 38 HU) compared with MRI (SII, from 0.35 to 6.37%).

Figure 6 ROC curves indicate the sensitivity, specificity, PPV and negative predictive value (NPV), and diagnostic accuracy (percentages are referred to findings) of ADC-based differentiation between groups (A versus B) for CT (a) and MRI (b). For each curve, the optimal cut-off value is highlighted with the relative values of sensitivity, specificity, PPV and NPV, and diagnostic accuracy.